Polímeros
ISSN 1678-5169 (Online)

https://doi.org/10.1590/0104-1428.20230031

ORIGINAL ARTICLE

Development and characterization of chitosan-collagen films loaded with honey

David Servín de la Mora-López[1], Tomás Jesús Madera-Santana[1]*, Jaime López-Cervantes[2]*, Dalia Isabel Sánchez-Machado[2], Jesús Fernando Ayala-Zavala[1] and Herlinda Soto-Valdez[1]

[1]Coordinación de Alimentos de Orígen Vegetal, Centro de Investigación en Alimentación y Desarrollo, Hermosillo, Sonora, México

[2]Laboratorio de Biotecnología y Ciencias Alimentarias, Instituto Tecnológico de Sonora, Ciudad Obregón, Sonora, México

**madera@ciad.mx; jaime.lopez@itson.mx*

Abstract

Biomaterials developed with biopolymers contribute to the healing process of healthy or diabetic patients. The objective of the present study was to evaluate the effect of honey incorporation (0.3, 0.6, and 1.2 g/100 mL) in chitosan/collagen/glycerol composite films. The Ch/Coll/1.2H films revealed the greatest percentage of elongation (27.10%) and Young´s modulus (65.58 MPa). The barrier properties (WVTR and WVP) exhibited a significant increase when the honey was incorporated into the films. The absorption capacity, solubility, and enzymatic biodegradability were lower in films containing honey. The chemical interactions between the functional groups of the films were verified by FTIR. The morphology studied by SEM confirmed the mixture's homogeneity. Finally, all formulations exhibited antibacterial properties against *Staphylococcus aureus*, *Pseudomonas aeruginosa*, *Listeria monocytogenes*, and *Salmonella Typhimurium*. The aforementioned properties of formulated dressings are suitable for their potential application in chronic wounds.

Keywords: *chitosan, collagen, Apis mellifera, antibacterial films, bioactive films.*

How to cite: Servín de la Mora-López, D., Madera-Santana, T. J., López-Cervantes, J., Sánchez-Machado, D. I., Ayala-Zavala, J. F., & Soto-Valdez, H. (2023). Development and characterization of chitosan-collagen films loaded with honey. *Polímeros: Ciência e Tecnologia*, *33*(3), e20230028. https://doi.org/10.1590/0104-1428.20230031

1. Introduction

Wounds are skin breaks caused by physical or thermal damage that can alter the physiological and bodily functions of the underlying tissue[1]. They can be classified as acute or chronic[2]. Chronic wounds affect a great part of the world's population. Their prevalence has increased with the growth of the adult population and comorbidities such as obesity and diabetes[2]. It has been estimated that around 1 to 2% of the world's population has suffered or will experience chronic injuries[3,4]. The costs of treating chronic wounds have been extremely expensive. In the United States, around $20 billion is invested annually in the health sector, solely for that purpose[4]. Traditionally, several natural materials such as biopolymers, animal fats, vegetable fibers, honey pastes, cotton fabrics, lint, and gauze have been widely used in medicine for wound healing[5]. The ideal material for wound healing should provide an adequate moist environment, promote gas exchange, possess adequate mechanical properties for handling and manipulation, act as an efficient barrier against infectious microorganisms, be non-toxic, and promote efficient wound healing[6,7].

Chitosan is a biopolymer derived from the thermo-alkali deacetylation of chitin, which is abundantly found in the exoskeletons of crustaceans and insects and in fungal cell walls[8]. The chitosan-free amino groups impart relevant properties such as antimicrobial, biodegradable, biocompatible, and non-toxic characteristics. These properties have served as a basis for providing an efficient treatment for several chronic conditions, such as diabetic foot, third-degree burns, decubitus ulcers, pyoderma gangrenosum, venous ulcers, and pressure ulcers[9].

Collagen is the main extracellular matrix (ECM) component that creates highly organized and elastic structures and confers physical tissue support[10]. It shows potential uses in biomedicine due to its ability to stimulate fibroblast and keratinocyte proliferation and promote the synthesis of proteins that make up the ECM[6,10]. Using additional collagen from external media allows for accelerated healing processes, including in wounds where healing occurs more slowly.

Honey has long been employed in traditional medicine as an effective therapy to treat burn injuries and chronic wounds[11]. The presence of flavonoids and phenolic compounds has favored the antioxidant roles of honey, which provide anti-inflammatory responses in wounds[12]. In addition, the antimicrobial nature of honey is directly associated with its supersaturated concentration of sugars, its high osmolarity in conjunction with its acidic nature, and the presence of hydrogen peroxides and flavonoids[13,14]. Honey can be

considered a suitable material because it decreases pain and swelling, and promotes autolytic debridement and healing[14].

The present study was focused on preparing chitosan/collagen/glycerol/honey films. The effect of incorporating honey at different concentrations in chitosan/collagen/glycerol films was evaluated. The optical, physicochemical, mechanical, barrier, structural, morphological, thermal, biodegradable, and antibacterial properties of the films were investigated to enhance their possible application as wound dressings.

2. Materials and Methods

2.1 Materials

Apis mellifera honey was acquired from a local market in Mani, Yuc. Mexico. The shrimp chitosan powder was supplied by Quitomex, S.A. (Obregon, Mexico). The chitosan has an average molecular weight of 378 KDa and a deacetylation degree of 87%. Hydrolyzed fish collagen was provided by the Food Science and Technology Laboratory at ITSON (Obregon, Mexico). Glycerol was purchased from REASOL (Mexico City, México). Glacial acetic acid was obtained from FAGALAB (Mocorito, Mexico). Lysozyme (40,000 units/mg) and phosphate-buffered saline (PBS) pH 7.4 were supplied by Sigma-Aldrich (St. Louis, MI, USA).

2.2 Preparation of chitosan-collagen-glycerol-honey-based films

Chitosan-collagen-honey composite films were prepared by the solution casting technique[15]. 100 mL of a solution of acetic acid (1% v/v) was used to prepare a composite blend of chitosan (1% w/v) and collagen (0.5% w/v). Both chitosan and collagen were mixed in the acetic acid solution. This mixture was considered a control group and named Ch/Coll. Based on this formulation, the other four blends were prepared by adding glycerol, and subsequently, honey at different concentrations, as described in Table 1. The solutions were homogenized by a magnetic stirrer, Cimarec™ Thermo Fisher Scientific (Waltham, MA, USA), at 25 ºC and subsequently filtered through 100 µm of organza fabric (100 mesh). Finally, the films were produced by pouring the corresponding solution into plastic containers (150 mL) and leaving them to dry at 45 ºC for 48 h in a DZF-6050 vacuum oven (Xiamen, China).

2.3 Optical properties of the films

Color determination of the films was performed using a colorimeter Chroma Meter CR-400, Konica Minolta (Osaka, Japan) calibrated to a standard (Y= 94.10, X= 0.3155, and y= 0.3319). Measurements were recorded at three specific points on the film, and an average of nine measurements was reported for each formulation. Using the CIELab scale, the values of L^* (lightness) and the chromatic parameters a^* (red/green) and b^* (yellow/blue) were measured. The color difference (ΔE) of each film was compared against the Ch/Coll formulation and was calculated using Equation 1:

$$\Delta E = \sqrt{(\Delta L^*)^2 + (\Delta a^*)^2 + (\Delta b^*)^2} \quad (1)$$

where $\Delta L^* = L - L_O$, $\Delta a^* = a - a_O$, and $\Delta b^* = b - b_O$. The L^*, a^*, and b^* parameters are the chromatic values of the sample, and L_O^*, a_O^*, and b_O^* represent the control's chromatic values (Ch/Coll film).

The transparency measurement was performed according to the methodology established by Escárcega-Galaz et al. [16]. Rectangular samples (3x1 cm) were made and placed inside a spectrophotometric cell. The absorbance readings were determined at 600 nm in a UV-Vis spectrophotometer Varian Cary 50 Bio. Transparency was calculated using the following Equation 2:

$$T = \frac{A_{600}}{t} \quad (2)$$

where A_{600} is the recorded absorbance value at 600 nm, and t represents the average thickness of the film in mm. The transparency of the films was analyzed, and the average value of two replicates was reported for each formulation.

2.4 Mechanical properties

The mechanical characterization of the films was analyzed using a texture analyzer TA-XT plus texture analyzer, Stable Micro Systems (Surrey, UK). The tensile parameters tensile strength (σ_{max}), elongation at break (ε_b), and Young's modulus (E) were calculated according to the ASTM D882-02 standard method[17]. Rectangular samples (10x60 mm) were obtained, and the thickness of each film was measured in triplicate. The separation distance, end-to-end, of 30 mm was set, and a 10 mm/min crosshead speed was programmed. The tensile parameters were reported based on the average value of six replicates per film.

2.5 Physicochemical properties

2.5.1 Water holding capacity and solubility

Water holding capacity (DS) and solubility (WS) tests were performed according to the methodology reported by Madera-Santana et al.[18]. with some modifications.

Table 1. Composition of films based on chitosan, collagen, glycerol, and honey.

Formulation	Ch[a] (g)	Coll[b] (g)	Gly[c] (g)	H[d] (g)
Ch/Coll	1.0	0.5	0	0
Ch/Coll/Gly	1.0	0.5	0.6	0
Ch/Coll/Gly/0.3H	1.0	0.5	0.6	0.3
Ch/Coll/Gly/0.6H	1.0	0.5	0.6	0.6
Ch/Coll/Gly/1.2H	1.0	0.5	0.6	1.2

[a]Ch: Chitosan. [b]Coll: Collagen. [c]Gly: Glycerol. [d]H: Honey. Solute (g/100 mL).

The films were evaluated with PBS pH 7.4 and deionized water. Circular cuts (3 mm in diameter) were performed in triplicate for each film formulation. The sample weight was recorded and transferred to a Petri dish. Subsequently, PBS or deionized water was added (3 mL), and the samples remained in adsorption equilibrium at different time intervals (5, 10, 15, 30, and 60 min). Excess moisture was removed by placing the film surface on filter paper. Finally, the weight of the wet sample was recorded, and the percentage of water retention was calculated using Equation 3:

$$\%DS = \frac{W_e - W_o}{W_o} \times 100 \quad (3)$$

where W_e corresponds to the weight of the film at equilibrium adsorption in PBS medium or deionized water, and W_o represents the initial weight of the film.

To determine solubility, wet samples employed for the %DS assay at time intervals of 60 min in both mediums were allowed to dry for 24 h. Solubility was calculated using Equation 4:

$$\%WS = \frac{W_o - W_d}{W_o} \times 100 \quad (4)$$

where W_o is the initial weight of the film and W_d is the weight of the film after the drying process at 60 ºC.

2.6 Barrier properties

2.6.1 Water Vapor Transmission Rate (WVTR)

The test to determine WVTR was performed according to the wet cup gravimetric method established by ASTM E96[19]. Water vapor diffusion was determined by the weight loss from a transmission container (*w*). For this purpose, a plastic container with deionized water (30 mL) was sealed with a lid containing the sample firmly fixed on its top. The container was stored at 25±1 °C and 30±5% RH in a desiccator with dry silica. The assay was performed in triplicate for each sample, and the container weight was recorded periodically for 30 h. WVTR was calculated from the slope of the straight line where time (h) vs. weight difference (g) was plotted using Equation 5:

$$WVTR = \frac{w}{t * A} \quad (5)$$

where *w* is the weight loss of the container (g), *t* is the time in hours and *A* corresponds to the permeation area ($2.85x10^{-4}$ m^2).

2.6.2 Water Vapor Permeability (WVP)

The determination of *WVP* was calculated from the *WVTR* and using Equation 6:

$$WVP = \frac{WVTR * l}{\Delta p} \quad (6)$$

where *l* is the average thickness of the film and Δp corresponds to the difference in water vapor pressure on the internal and external sides of the container where the film sample is located.

2.7 Fourier transform infrared spectroscopy (FTIR)

The infrared spectra of the samples were obtained using FTIR-ATR equipment Nicolet iS50 FTIR, Thermo Fisher Scientific (Waltham, MA, USA). The study was carried out in a wavenumber range from 4000 to 600 cm^{-1} with a spectral resolution of 4 cm^{-1}, and 64 scans were performed for each formulation.

2.8 Morphological and elemental analysis

Surface morphology was analyzed using micrographs taken in a field emission scanning electron microscope (FESEM) model JEOL JSM-7600F (Peabody, MA, USA). The samples were placed on an aluminum stub, and the observation was performed at an angle of 90º to the surface.

2.9 In vitro enzymatic biodegradation

The biodegradation study of the films was performed according to the methodology proposed by Martinez-Ibarra et al.[9] with some modifications. The assay was performed in a PBS solution containing lysozyme (40,000 units/mg) at a 2 mg/mL concentration. For this purpose, circular dry samples with diameters of 17 mm were weighed and immersed in a PBS solution containing lysozyme (3 mL). Samples were incubated at 37 °C for 9 days, and weight was determined at 1, 2, 4, 7, and 9 days. To carry out the measurements, the samples were removed from the enzyme solution and carefully washed with distilled water to interrupt the enzymatic process. The excess moisture was removed using filter paper, the films were dried, and their weight was recorded. *In vitro* enzymatic biodegradation was evaluated by weight loss, which was calculated by the following Equation 7:

$$\%Weight\ loss = \frac{W_o - W_t}{W_o} \times 100 \quad (7)$$

where W_o is the weight of the dry sample before contact with lysozyme and W_t is the weight of the sample after contact with the enzyme. The results corresponding to biodegradation were calculated based on an average of three replicates per formulation.

2.10 Antibacterial properties

The antibacterial properties of the films were evaluated against *Staphylococcus aureus* ATCC 6538, *Pseudomonas aeruginosa* ATCC 10154, *Listeria monocytogenes* ATCC 7644, and *Salmonella* Typhimurium ATCC 14028 using the method established by Rodríguez-Núñez et al.[15]. Inoculums were prepared 18 h before the study to reach their exponential phases; a loop of bacteria was introduced into tubes with BD Difco™ Mueller-Hinton broth (10 mL) and incubated at 37 °C. Small aliquots of each inoculum were transferred to tubes with saline solution (NaCl 0.9% w/v) until their absorbance was adjusted to 0.100 at 600 nm in UV/vis spectroscopy (equivalent to 10^8 CFU/mL). To evaluate the antibacterial properties of the films, 16 mm

Table 2. Optical properties of films based on chitosan and collagen loaded with honey.

Formulation	Color parameters				Transparency
	*L**	*a**	*b**	ΔE	
Ch/Coll	81.30 ± 0.47^{c}	-1.79 ± 0.08^{a}	35.31 ± 1.86^{c}	ND	1.54 ± 0.03^{b}
Ch/Coll/Gly	82.01 ± 0.30^{c}	-1.59 ± 0.07^{a}	34.23 ± 0.81^{bc}	4.96 ± 0.90^{a}	0.96 ± 0.02^{a}
Ch/Coll/Gly/0.3H	57.94 ± 2.75^{b}	24.92 ± 2.59^{b}	54.40 ± 2.13^{d}	36.17 ± 3.72^{b}	2.67 ± 0.21^{c}
Ch/Coll/Gly/0.6H	34.44 ± 1.47^{a}	32.33 ± 0.70^{c}	25.34 ± 0.95^{a}	57.13 ± 2.64^{c}	3.41 ± 0.21^{d}
Ch/Coll/Gly/1.2H	35.67 ± 3.05^{a}	33.27 ± 0.33^{c}	32.61 ± 2.81^{b}	54.45 ± 2.20^{c}	3.74 ± 0.15^{d}

Mean values ± standard deviation is reported for each treatment. ND: No determined. Different letters in the same column indicate significant difference (p<0.05).

diameter film samples were placed in tubes containing 10 mL of Mueller-Hinton broth. Then 10 µL of the adjusted inoculum was introduced. An inoculated tube without a film sample was used as a bacterial control for comparison. The samples were incubated at 37 °C for 24 h, and 200 µL of the broths were transferred to polypropylene microplate wells. Absorbance readings were performed at 600 nm on a UV-Vis SPECTROStar Omega microplate reader (BMG LabTech GmbH, Germany).

Finally, the colony-forming units (CFU/mL) were calculated from the absorbance obtained using the equations established by Gonzáles-Pérez et al.[20] (Supplementary Material).

2.11 Statistical analysis

A completely randomized design was used, where the response variables were measured according to the composition of glycerol (0 and 0.6 g/100 mL) and honey (0, 0.3, 0.6, and 1.2 g/100 mL) in the films. The Ch/Coll films were considered control samples. The mean values ± standard deviations of the replicates were reported for each analysis. An analysis of variance (ANOVA) test was performed using the STATGRAPHICS PLUS 5.1 statistical package. Statistically significant differences between the means of each group were estimated below a significance level of (p<0.05).

3. Results and Discussions

3.1 Optical properties

The color parameters of the Ch/Coll, Ch/Coll/Gly, and Ch/Coll/Gly/H films are listed in Table 2. The Ch/Coll/Gly films did not generate changes in *L** and *a** compared to the Ch/Coll films. In qualitative terms, the Ch/Coll films showed a clear yellow, homogeneous, and transparent coloration, while the addition of glycerol conferred a mostly shiny and smooth surface texture. In contrast, brown coloration was observed due to honey addition in the films (Figure SI1, Supplementary Material). The *a** values exhibited low blue tinting in the Ch/Coll films, while reddening appeared in the honey composite films. The *b** value showed yellowness in all films, with the Ch/Coll/Gly/0.3H formulation exhibiting the strongest yellow tint. The color difference (ΔE) revealed statistical differences among the films (p<0.05). The lowest values corresponded to the Ch/Coll/Gly formulation, while the Ch/Coll/40Gly/0.6H films had the highest color difference according to the control film (Ch/Coll film). The browning by the honey Maillard reactions generated a greater reddening and decreased lightness (*L**) that caused an increment in ΔE. Significant changes were obtained by Escárcega-Galaz et al.[16], who reported significant increases in *L**, *a**, and ΔE by including honey and glycerol compounds in their chitosan films, which showed a trend very similar to those reported here.

Table 3. Mechanical properties of films based on chitosan and collagen loaded with honey.

Formulation	σ_{max}	ε_b	E
	[MPa]	[%]	[MPa]
Ch/Coll	71.78 ± 5.5^{d}	1.66 ± 0.3^{a}	3882.7 ± 1007.2^{c}
Ch/Coll/Gly	24.74 ± 6.9^{b}	8.51 ± 1.9^{c}	722.5 ± 181.9^{b}
Ch/Coll/Gly/0.3H	19.84 ± 5.1^{b}	2.94 ± 1.2^{ab}	974.9 ± 310.5^{b}
Ch/Coll/Gly/0.6H	33.06 ± 9.5^{c}	4.30 ± 1.4^{b}	1110.3 ± 192.1^{b}
Ch/Coll/Gly/1.2H	8.61 ± 1.7^{a}	27.10 ± 2.3^{d}	65.6 ± 12.9^{a}

Mean values ± standard deviation are reported for each treatment. Different letters in the same column indicate a significant difference (p<0.05).

Table 2 illustrates the corresponding transparency of the analyzed formulations. Transparency ranged from 0.96 to 3.74, with the Ch/Coll/Gly films having the lowest transparency value, while the Ch/Coll/Gly/1.2H films exhibited the highest values. The inclusion of glycerol significantly decreased (p<0.05) the transparency values in the Ch/Coll films. This effect was confirmed by Rivero et al.[21], where they evidenced that the presence of glycerol improved transparency in laminated films based on gelatin/chitosan.

3.2 Mechanical properties

In this study, the mechanical parameters measured in the films by the tensile test were determined by the stress-strain curves. These parameters, tensile strength (σ_{max}), elongation at break (ε_b), and Young's modulus (E), are shown in Table 3. The σ_{max} of the films presented ranges that fluctuated between 8.61 MPa and 71.78 MPa; the ε_b ranged from 1.66% to 27.10%; and the E showed values between 65.58 MPa and 3882.73 MPa. The Ch/Coll films exhibited the highest values of σ_{max} and E, although they exhibited the lowest value of ε_b. This film formulation had high strength, but it was not flexible and showed brittle characteristics.

The incorporation of glycerol into Ch/Coll films produced a significant decrease (p<0.05) in σ_{max} and E values. In contrast, the ε_b showed a significant increase (p<0.05). This combination of results was mainly pronounced in formulations that contained honey. The most noticeable

changes were observed in the Ch/Coll/Gly/1.2H film, which provided mostly elastic and flexible structures. These characteristics were attributed to the capability of glycerol and honey to act as plasticizing agents in the films. Recently, Rocha-Lemus et al.[22] reported the performance of honey as a plasticizer in graphene oxide-agar films. Other authors have reported that incorporating glycerol and honey can promote a larger free volume between the polymeric chains, causing a decrease in the intermolecular interactions among them[15]. It explains the drastic decreases in elastic modulus values and the increase in elongation rates when both compounds were added to Ch/Coll films, particularly in the Ch/Coll/Gly/1.2H formulation. On the other hand, the Ch/Coll/Gly/0.3H and Ch/Coll/Gly/0.6H films revealed lower elongation at break and a higher elastic modulus compared to Ch/Coll/Gly films but were more elastic and flexible when compared to Ch/Coll films.

3.3 Physicochemical properties

3.3.1 Water holding capacity and solubility

Figure 1 shows the kinetics of the water-holding capacity performed on each film for 60 min using PBS solution and deionized water as hydrating agents, both at 25 ºC. The study revealed that all formulations reached equilibrium absorption after 15 min of contact with the PBS solution (Figure 2a). However, the instability in the behavior of the Ch/Coll/Gly formulation was observed between 5 and 10 min, while in the Ch/Coll/Gly/0.3H film, there was a fluctuation between 10 and 15 min. The film that exhibited the highest adsorption capacity in PBS was Ch/Coll, with a retention rate of 111.79% at 5 min and 67.96% at 60 min of contact. In contrast, the Ch/Coll/Gly/0.6H formulation revealed the lowest rates, measured at 32.05% and 6.63% at 5 and 60 min, respectively.

Figure 1b revealed the water-holding capacity of films hydrated with deionized water. The kinetics indicated that the films, except for Ch/Coll/Gly, achieved equilibrium adsorption after being in contact for 10 min with the hydrating medium. The Ch/Coll/Gly films exhibited a considerable increase in their adsorption with values between 5 and 30 min; however, at these times, they achieved equilibrium. The highest absorption rates corresponded to the Ch/Coll formulation, and the film with the lowest water retention was the Ch/Coll/Gly/1.2H formulation. Likewise, the study indicated no considerable differences in the values obtained among the films containing honey. The decrease in water-holding capacity in honey composite films is an effect associated with the hydrophilic nature of honey and the viscosity of the polymers used to produce the films. Likewise, honey can restrict mobility and free rotation among polymer chains by forming strong hydrogen-bonding interactions with chitosan, collagen, and glycerol due to the presence of many functional groups among the components. In this sense, strong interactions between polymers could shorten intermolecular distances and create a much more compact network, resulting in a lower adsorption capacity. Figure SI2 (Supplementary Material) shows the solubility of the different formulations exposed for 60 min in PBS solution and deionized water.

3.4 Barrier properties

Figure 2 shows the water permeability behavior for each formulation described. The film's water vapor diffusion was significantly affected by incorporating glycerol and honey. According to Figure 2, the Ch/Coll/Gly/0.3H films exhibited the highest WVTR and WVP values; in contrast, the Ch/Coll films presented the lowest WVTR and WVP. The Ch/Coll/Gly films exhibited higher WVTR and WVP in comparison to the Ch/Coll films. Ziani et al.[23] obtained increases in their WVP values from 0.89 to 1.11 g mm kPa^{-1} h^{-1} m^{-2} when plasticizing chitosan films (96% DD) with glycerol. It can be explained because glycerol possesses short linear chains that allow it to incorporate into adjacent polymeric chains, increasing the free volume and weakening the intermolecular forces. This effect causes the polymeric network to be less dense and favors greater water vapor molecules diffusion.

The honey inclusion promoted significant increases in film permeability. However, no significant differences (p>0.05) were found for WVTR in Ch/Coll/Gly/0.3H and

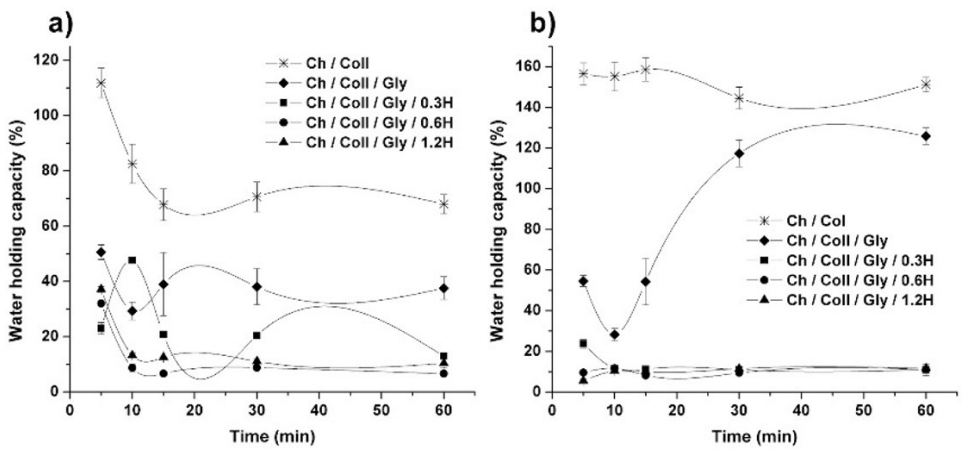

Figure 1. Kinetics of water-holding capacity of films based on chitosan and collagen loaded with honey hydrated with PBS (a) and deionized water (b).

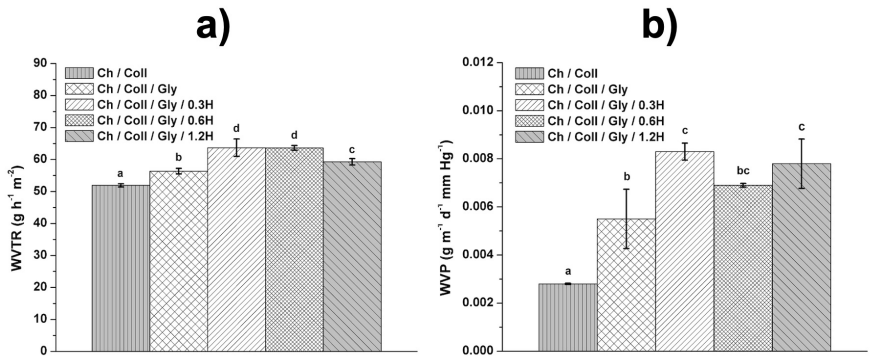

Figure 2. WVTR (a) and WVP (b) of films based on chitosan and collagen loaded with honey. Different letters in each column indicate a significant difference (p<0.05).

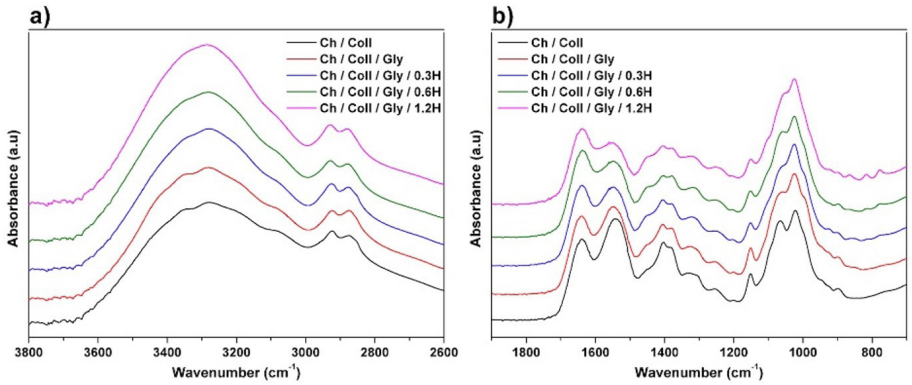

Figure 3. FTIR-ATR spectra of films based on chitosan and collagen loaded with honey at wavelengths 2600 - 3800 cm^{-1} (a) and 700 – 1900 cm^{-1} (b).

Ch/Coll/Gly/0.6H films. Likewise, statistical similarities (p>0.05) were found for WVP in Ch/Coll/Gly/0.3H and Ch/Coll/Gly/1.2H films. Slight decreases in permeability behavior with increasing honey concentrations in the films were observed. During the healing process, biomaterials must control water loss in the wound at optimal levels and provide adequate moisture to prevent excessive dehydration and facilitate tissue healing. Considering these criteria, Ch/Coll/Gly/0.6H films had a lower WVP, which results in the formulations with the best properties to prevent dehydration and maintain suitable wound environments.

3.5 FTIR analysis

The effects of the interactions of the chitosan-collagen films and the subsequent incorporation of glycerol and honey were evaluated by FTIR spectroscopy (Figure 3).

The absorption patterns of the Ch/Coll films revealed extensive bands at 3358–3276 cm^{-1} attributed to N-H bonds stretching vibrations and the existence of O-H groups linked by hydrogen bonds[24]. The signals found at lengths of 2923–2873 cm^{-1} were associated with the stretching vibrations of C-H groups contained in chitosan and collagen molecules. The absorption band related to Amide I, corresponding to C=O group stretching vibrations, was located at 1637 cm^{-1}. The Amide II was found at 1541 cm^{-1} and was attributed to the C-N group stretching vibrations in conjunction with N-H and CH_2 bending vibrations[25]. The collagen's O-H deformation (COOH) was found at 1401 cm^{-1}. An extensive absorption band between 1199 and 1022 cm^{-1} showed the C-O stretching vibration, which is characteristic of the polysaccharide structure of chitosan. Specifically, the peak located at 1151 cm^{-1} corresponded to C-O-C bond stretching vibrations, and the peaks found at 1065 cm^{-1} and 1022 cm^{-1} were related to C-O bond vibrations. The absorption band associated with the pyranose ring stretching of chitosan was found at 899 cm^{-1}[24].

FTIR analysis showed overlaps of the O-H groups over the N-H groups at 3278 cm^{-1}. This effect explains the strong stretching vibration of the O-H groups of chitosan, collagen, glycerol, and honey[26]. Higher absorption intensities were found at 2923-2873 cm^{-1}, corresponding to C-H groups of carboxylic acids and NH_3^+ groups of free amino acids, indicating the presence of honey in the films. The most notable changes in the spectra occurred with the appearance of a strong Amide I band, whose peak was augmented with increasing honey concentration in the films.

Likewise, the honey incorporation decreased the absorption bands of Amide II, and the peak was found at 1401 cm^{-1} (O-H

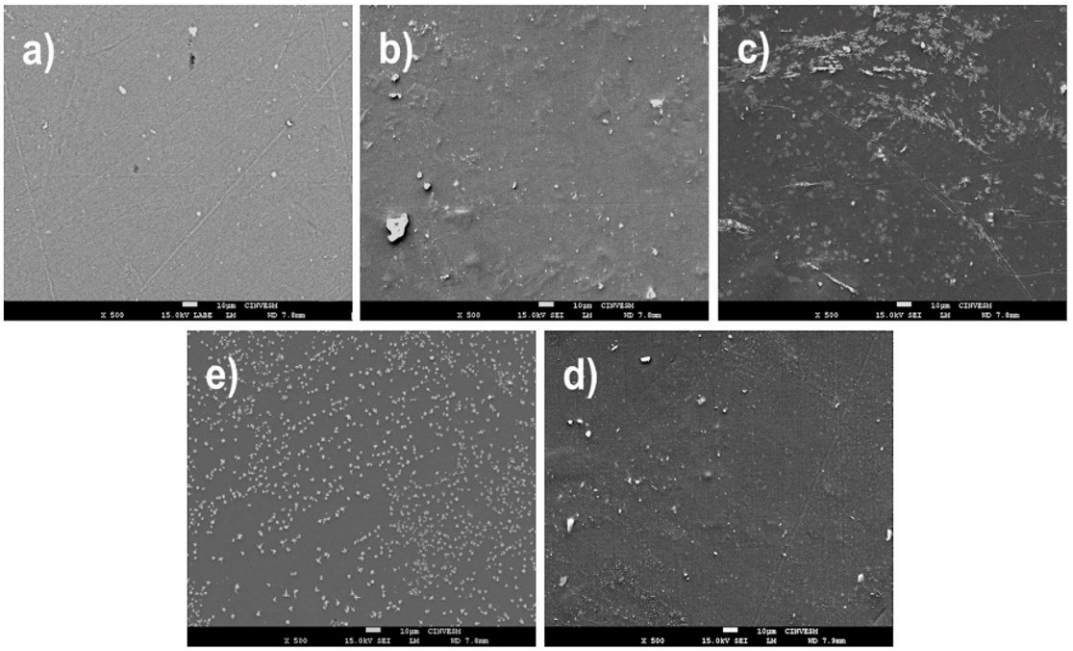

Figure 4. SEM micrographs of films based on chitosan and collagen: Ch/Coll (a), Ch/Coll/Gly (b), Ch/Coll/Gly/0.3H (c), Ch/Coll/Gly/0.6H (d), and Ch/Coll/Gly/1.2H (e).

deformation). These changes could indicate a possible interaction of hydrogen bonds between the COOH, NH_2, C=O, and OH groups found in the film's components[26,27]. The glycerol addition caused an overlap at 1023 cm^{-1}, and its intensity increased with the addition of honey. The signal at wavenumbers between 700-940 cm^{-1} is attributed to bending vibrations of the honey carbohydrate ring in anomeric regions, while at wavenumbers from 940 to 1145 cm^{-1}, it is due to the C-C and C-O groups stretching the carbohydrates.

3.6 Morphological analysis

The surface morphology of the films was analyzed by SEM micrographs, as shown in Figure 4. The test was performed under a magnification of 500x at a scale of 10 µm. The study revealed films with smooth, homogeneous, and continuous surfaces, indicating that the components were uniformly dispersed in the polymer matrix. However, it was possible to witness some rough regions in the Ch/Coll/Gly and Ch/Coll/Gly/0.6H films. In addition, all films exhibited good structural integrity with the absence of porosities, cracks, or fractures on their surfaces. Micrographs revealed good miscibility in Ch/Coll and Ch/Coll/Gly films; however, small crystals started to appear with the incorporation of honey into the membranes. Costa et al.[28] mentioned that this phenomenon is strongly related to glucose, which can favor honey crystallization during storage due to its presence at supersaturated concentrations. The low solubility of glucose in water allows these molecules to separate from water and form crystals, as shown in Figures 4c, 4d, and 4e.

3.7 In vitro enzymatic biodegradation

The films presented successive weight losses as a consequence of the dynamic degradation of lysozyme,

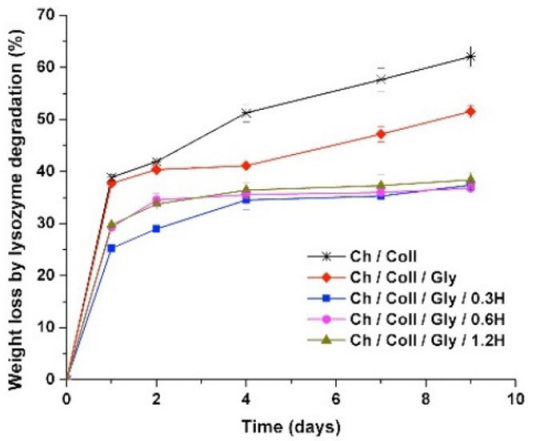

Figure 5. Kinetic of enzymatic degradation by lysozyme in films based on chitosan and collagen loaded with honey.

as shown in Figure 5. The largest weight loss in the films occurred during the first day of incubation. After nine days, Ch/Coll and Ch/Coll/Gly films were completely dissolved in the enzyme-containing solution, while formulations of Ch/Coll/Gly/0.3H, Ch/Coll/Gly/0.6H, and Ch/Coll/Gly/1.2H presented breakage to small particles as a consequence of hydrolysis. The Ch/Coll formulation showed the highest biodegradability rate, with weight losses of 62.10%. The Ch/Coll/Gly films showed very similar behaviors during the first two days of incubation; however, after day four, a lower weight loss was observed compared to the Ch/Coll films.

On the other hand, the honey incorporation in the films had a less pronounced effect. The Ch/Coll/Gly/0.6H formulation

recorded the lowest weight loss with values of 36.79% at nine days of incubation. Similarly, the Ch/Coll/Gly/0.3H films revealed higher progressive weight losses over the first four days of incubation but no significant differences (p>0.05) between the honey-based formulations. The above results indicated that glycerol and honey favored lower weight loss. Moreover, there was a direct relationship between the biodegradability of the films and their adsorption capacity. The Ch/Coll and Ch/Coll/Gly formulations presented the highest biodegradability rates because they had a higher capacity to absorb the enzymatic solution, which favored contact with a greater volume of lysozyme in the films.

3.8 Antibacterial properties

The antibacterial activity of films based on chitosan and collagen loaded with honey is given in Figure 6. Significant reductions (p<0.05) were observed in all formulations compared to the control for each microorganism. When the films were evaluated against *S. aureus*, some significant differences (p<0.05) were observed among the treatments employed. The Ch/Coll films presented the highest bacterial reduction of all films ($1.57x10^8$ CFU/mL), while the Ch/Coll/Gly/0.3H formulation revealed the highest microbial count ($2.87x10^8$ CFU/mL). The effect of honey, according to the increase in its concentration on the films, caused gradual decreases in the microbial count of *S. aureus*.

On the other hand, films inoculated with *P. aeruginosa* presented a different behavior in their microbial growth. The Ch/Coll composite films exhibited the highest counts with values of $1.31x10^8$ CFU/mL, and the lowest count was recorded for the Ch/Coll/Gly/0.3H formulation ($8.48x10^7$ CFU/mL). Increasing the honey concentration in the films caused increases in their microbial counts. For *L. monocytogenes* and *S.* Typhimurium, similar trends were observed among the different treatments. The microbial count values gradually decreased as honey was incorporated and concentrations increased. In both study organisms, statistical similarities (p<0.05) were observed between the counts of Ch/Coll and Ch/Coll/Gly films. In contrast, the effect of honey showed significant differences (p<0.05) when compared in both films.

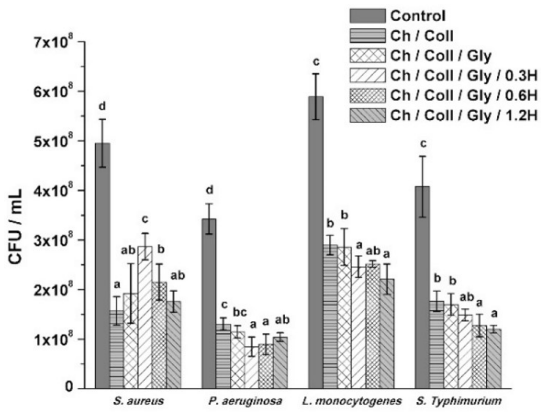

Figure 6. Antibacterial activity of films based on chitosan and collagen loaded with honey against *S. aureus*, *P. aeruginosa*, *L. monocytogenes*, and *S.* Typhimurium. Different letters in each group of columns per bacteria indicate a significant difference (p<0.05).

Both chitosan and honey are compounds that contribute synergistically to the antibacterial properties of the films. The antibacterial properties of honey lie in its supersaturated concentration of sugars, its high osmolarity, its acidic nature, the constant production of hydrogen peroxides, and the existence of lysozymes, phenolic acid, and flavonoids[13,14]. In contrast, chitosan with positively charged amino groups can interact with the negatively charged bacterial cell wall. This process produces strong electrostatic interactions, resulting in cell wall rupture and leakage of intracellular components, causing cell death[28,29]. In addition, many studies have shown that chitosan can block the cell membrane of Gram+ bacteria and prevent the entry of nutrients into the cell[30].

4. Conclusions

Honey is a favorable compound to be incorporated into biomaterials. In this work, films of chitosan, collagen, glycerol, and honey were prepared by using the solution casting technique. All the films were transparent and presented a good appearance and color in their structure. Additionally, the interactions between the functional groups of the compounds used in this study allowed the formation of miscible, homogeneous, and uniformly dispersed mixtures. The effect of honey on the films promoted increases in elongation at break and tear strength, generating mostly flexible and elastic films. The enzymatic biodegradation of films by lysozyme action resulted in lower weight losses in the films containing honey. In addition, this research demonstrated that the films had enhanced antibacterial properties against *S. aureus*, *P. aeruginosa*, *L. monocytogenes*, and *S.* Typhimurium when honey was incorporated into them. These results reveal that honey-prepared films are a promising alternative for chronic wound treatment in biomedicine.

5. Author's Contribution

- **Conceptualization –** Tomás Jesús Madera-Santana; Jaime López-Cervantes; Dalia Isabel Sánchez-Machado; Herlinda Soto-Valdez; Jesús Fernando Ayala-Zavala.
- **Data curation** – David Servín de la Mora-López; Tomás Jesús Madera-Santana.
- **Formal analysis** – David Servín de la Mora-López.
- **Funding acquisition** – Tomás Jesús Madera-Santana.
- **Investigation** – David Servín de la Mora-López.
- **Methodology** – David Servín de la Mora-López; Tomás Jesús Madera-Santana.
- **Project administration** – Tomás Jesús Madera-Santana.
- **Resources** – Tomás Jesús Madera-Santana; Jaime López-Cervantes; Dalia Isabel Sánchez-Machado; Herlinda Soto-Valdez; Jesús Fernando Ayala-Zavala.
- **Software** – NA
- **Supervision** – Tomás Jesús Madera-Santana; Jaime López-Cervantes; Dalia Isabel Sánchez-Machado; Herlinda Soto-Valdez; Jesús Fernando Ayala-Zavala.

• **Validation** – NA.

• **Visualization** – Tomás Jesús Madera-Santana; Jaime López-Cervantes.

• **Writing – original draft** – David Servín de la Mora-López.

• **Writing – review & editing** – Tomás Jesús Madera-Santana; Jaime López-Cervantes; Dalia Isabel Sánchez-Machado; Herlinda Soto-Valdez; Jesús Fernando Ayala-Zavala.

6. Acknowledgements

David Servín de la Mora López would like to thank to CONACyT for the scholarship granted for his doctoral studies. Part of this research was conducted at the facilities of Laboratorio Nacional CONACYT LANNBIO-Cinvestav Unidad Mérida (PROY. No. 321119).

7. References

1. Torres, F. G., Commeaux, S., & Troncoso, O. P. (2013). Starch-based biomaterials for wound-dressing applications. *Starch*, *65*(7-8), 543-551. http://dx.doi.org/10.1002/star.201200259.
2. Yaşayan, G., Karaca, G., Akgüner, Z. P., & Bal-Öztürk, A. (2021). Chitosan/collagen composite films as wound dressings encapsulating allantoin and lidocaine hydrochloride. *International Journal of Polymeric Materials and Polymeric Biomaterials*, *70*(9), 623-635. http://dx.doi.org/10.1080/00914037.2020.1740993.
3. Sun, B. K., Siprashvili, Z., & Khavari, P. A. (2014). Advances in skin grafting and treatment of cutaneous wounds. *Science*, *346*(6212), 941-945. http://dx.doi.org/10.1126/science.1253836. PMid:25414301.
4. Järbrink, K., Ni, G., Sönnergren, H., Schmidtchen, A., Pang, C., Bajpai, R., & Car, J. (2016). Prevalence and incidence of chronic wounds and related complications: A protocol for a systematic review. *Systematic Reviews*, *5*(1), 152. http://dx.doi.org/10.1186/s13643-016-0329-y. PMid:27609108.
5. Mir, M., Ali, M. N., Barakullah, A., Gulzar, A., Arshad, M., Fatima, S., & Asad, M. (2018). Synthetic polymeric biomaterials for wound healing: a review. *Progress in Biomaterials*, *7*(1), 1-21. http://dx.doi.org/10.1007/s40204-018-0083-4. PMid:29446015.
6. Xie, H., Chen, X., Shen, X., He, Y., Chen, W., Luo, Q., Ge, W., Yuan, W., Tang, X., Hou, D., Jiang, D., Wang, Q., Liu, Y., Liu, Q., & Li, K. (2018). Preparation of chitosan-collagen-alginate composite dressing and its promoting effects on wound healing. *International Journal of Biological Macromolecules*, *107*, 93-104. http://dx.doi.org/10.1016/j.ijbiomac.2017.08.142.
7. Raisi, A., Asefnejad, A., Shahali, M., Doozandeh, Z., Moghadas, B. K., Saber-Samandari, S., & Khandan, A. (2020). A soft tissue fabricated using a freeze-drying technique with carboxymethyl chitosan and nanoparticles for promoting effects on wound healing. *Journal of Nanoanalysis*, *7*(4), 262-274. http://dx.doi.org/10.22034/JNA.2022.680836.
8. Wu, J., Su, C., Jiang, L., Ye, S., Liu, X., & Shao, W. (2018). Green and facile preparation of chitosan sponges as potential wound dressings. *ACS Sustainable Chemistry & Engineering*, *6*(7), 9145-9152. http://dx.doi.org/10.1021/acssuschemeng.8b01468.
9. Martínez-Ibarra, D. M., Sánchez-Machado, D. I., López-Cervantes, J., Campas-Baypoli, O. N., Sanches-Silva, A., & Madera-Santana, T. J. (2018). Hydrogel wound dressings based on chitosan and xyloglucan: development and characterization. *Journal of Applied Polymer Science*, *136*(12), 47342. http://dx.doi.org/10.1002/app.47342.
10. Valencia-Gómez, L. E., Martel-Estrada, S. A., Vargas-Requena, C. L., Rodriguez-González, C. A., & Olivas-Armendariz, I. (2016). Apósitos de polímeros naturales para regeneración de piel. *Revista Mexicana de Ingeniería Biomédica*, *37*(3), 235-249. http://dx.doi.org/10.17488/rmib.37.3.4.
11. Majtan, J. (2014). Honey: an immunomodulator in wound healing. *Wound Repair and Regeneration*, *22*(2), 187-192. http://dx.doi.org/10.1111/wrr.12117. PMid:24612472.
12. El-Kased, R. F., Amer, R. I., Attia, D., & Elmazar, M. M. (2017). Honey-based hydrogel: *in vitro* and comparative *In vivo* evaluation for burn wound healing. *Scientific Reports*, *7*(1), 9692. http://dx.doi.org/10.1038/s41598-017-08771-8. PMid:28851905.
13. Shamloo, A., Aghababaie, Z., Afjoul, H., Jami, M., Bidgoli, M. R., Vossoughi, M., Ramazani, A., & Kamyabhesari, K. (2021). Fabrication and evaluation of chitosan/gelatin/PVA hydrogel incorporating honey for wound healing applications: An *in vitro, in vivo* study. *International Journal of Pharmaceutics*, *592*, 120068. http://dx.doi.org/10.1016/j.ijpharm.2020.120068. PMid:33188894.
14. Sarhan, W. A., & Azzazy, M. H. M. (2015). High concentration honey chitosan electrospun nanofibers: biocompatibility and antibacterial effects. *Carbohydrate Polymers*, *122*, 135-143. http://dx.doi.org/10.1016/j.carbpol.2014.12.051. PMid:25817652.
15. Rodríguez-Núñez, J. R., Madera-Santana, T. J., Sánchez-Machado, D. I., López-Cervantes, J., & Soto-Valdez, H. (2014). Chitosan/hydrophilic plasticizer-based films: Preparation, physicochemical and antimicrobial properties. *Journal of Polymers and the Environment*, *22*(1), 41-51. http://dx.doi.org/10.1007/s10924-013-0621-z.
16. Escárcega-Galaz, A. A., Sánchez-Machado, D. I., López-Cervantes, J., Sanches-Silva, A., Madera-Santana, T. J., & Paseiro-Losada, P. (2018). Mechanical, structural and physical aspects of chitosan-based films as antimicrobial dressings. *International Journal of Biological Macromolecules*, *116*, 472-481. http://dx.doi.org/10.1016/j.ijbiomac.2018.04.149. PMid:29727650.
17. American Society for Testing and Materials. (2002). *ASTM D882-02: standard test method for tensile properties of thin plastic sheeting*. West Conshohocken, PA: ASTM.
18. Madera-Santana, T. J., Freile-Pelegrín, Y., & Azamar-Barrios, J. A. (2014). Physicochemical and morphological properties of plasticized poly(vinyl alcohol)–agar biodegradable films. *International Journal of Biological Macromolecules*, *69*, 176-184. http://dx.doi.org/10.1016/j.ijbiomac.2014.05.044. PMid:24875313.
19. American Society for Testing and Materials. (2010). *ASTM E96/E96M-10: standard test methods for water wapor transmission of materials*. Philadelphia, PA: ASTM.
20. González-Pérez, C. J., Tanori-Cordova, J., Aispuro-Hernández, E., Vargas-Arispuro, I., & Martínez-Téllez, M. A. (2019). Morphometric parameters of foodborne related-pathogens estimated by transmission electron microscopy and their relation to optical density and colony forming units. *Journal of Microbiological Methods*, *165*, 105691. http://dx.doi.org/10.1016/j.mimet.2019.105691. PMid:31437554.
21. Rivero, S., Garcia, M. A., & Pinotti, A. (2009). Composite and bi-layer films based on gelatin and chitosan. *Journal of Food Engineering*, *90*(4), 531-539. http://dx.doi.org/10.1016/j.jfoodeng.2008.07.021.
22. Rocha-Lemus, L. M., Azamar-Barrios, J. A., Ortíz-Vazquez, E., Quintana-Owen, P., Freile-Pelegrín, Y., Gamboa-Perera, F., & Madera-Santana, T. J. (2021). Development and physical characterization of novel bio-nanocomposite films based on reduced graphene oxide, agar and melipona honey. *Carbohydrate Polymer Technologies and Applications*, *2*, 100133. http://dx.doi.org/10.1016/j.carpta.2021.100133.

23. Ziani, K., Oses, J., Coma, V., & Maté, J. I. (2008). Effect of the presence of glycerol and Tween 20 on the chemical and physical properties of films based on chitosan with different degree of deacetylation. *Food Science and Technology (Campinas)*, *41*(10), 2159-2165. http://dx.doi.org/10.1016/j.lwt.2007.11.023.
24. Amiri, N., Moradi, A., Tabasi, S. A. S., & Movaffagh, J. (2018). Modeling and process optimization of electrospinning of chitosan-collagen nanofiber by response surface methodology. *Materials Research Express*, *5*(4), 045404. http://dx.doi.org/10.1088/2053-1591/aaba1d.
25. Shah, R., Stodulka, P., Skopalova, K., & Saha, P. (2019). Dual crosslinked collagen/chitosan film for potential biomedical applications. *Polymers*, *11*(12), 2094. http://dx.doi.org/10.3390/polym11122094. PMid:31847318.
26. Samadieh, S., & Sadri, M. (2021). Preparation and Biomedical properties of transparent chitosan/gelatin/honey/aloe vera nanocomposite. *Nanomedicine Research Journal*, *5*(1), 1-12. http://dx.doi.org/10.22034/nmrj.2020.01.001.
27. Campa-Siqueiros, P., Madera-Santana, T. J., Ayala-Zavala, J. F., López-Cervantes, J., Castillo-Ortega, M. M., & Herrera-Franco, P. J. (2020). Nanofibers of gelatin and polyvinyl-alcohol-chitosan for wound dressing application: fabrication and characterization. *Polímeros: Ciência e Tecnologia*, *30*(1), e2020006. http://dx.doi.org/10.1590/0104-1428.07919.
28. Costa, L. C. V., Kaspchak, E., Queiroz, M. B., Almeida, M. M., Quast, E., & Quast, L. B. (2015). Influence of temperature and homogenization on honey crystallization. *Brazilian Journal of Food Technology*, *18*(2), 155-161. http://dx.doi.org/10.1590/1981-6723.7314.
29. Raisi, A., Asefnejad, A., Shahali, M., Kazerouni, Z. A. S., Kolooshani, A., Saber-Samandari, S. S., Moghadas, B. K., & Khandan, A. (2020). Preparation, characterization, and antibacterial studies of N, O-carboxymethyl chitosan as a wound dressing for bedsore application. *Archives of Trauma Research*, *9*(4), 181-188. http://dx.doi.org/10.4103/atr.atr_10_20.
30. Radoor, S., Karayil, J., Jayakumar, A., Siengchin, S., & Parameswaranpillai, J. (2021). A low cost and eco-friendly membrane from polyvinyl alcohol, chitosan and honey: synthesis, characterization and antibacterial property. *Journal of Polymer Research*, *28*(3), 82. http://dx.doi.org/10.1007/s10965-021-02415-2.

Received: May 29, 2023
Revised: Aug. 12, 2023
Accepted: Aug. 17, 2023

Supplementary Material

Supplementary material accompanies this paper.

Supplementary information

Figure SI1. Chitosan-collagen films loaded with honey.

Figure SI2. Solubility of films based on chitosan and collagen loaded with honey in PBS solution and deionized water. Different letters in each column indicate a significant difference ($p<0.05$).

This material is available as part of the online article from https://doi.org/10.1590/0104-1428.20230031